

A complementary study of simulations and experiments to characterize the mean structure of the recirculatory flow at the rear of a 3D blunt body at different attitudes

Olivier Cadot
University of Liverpool

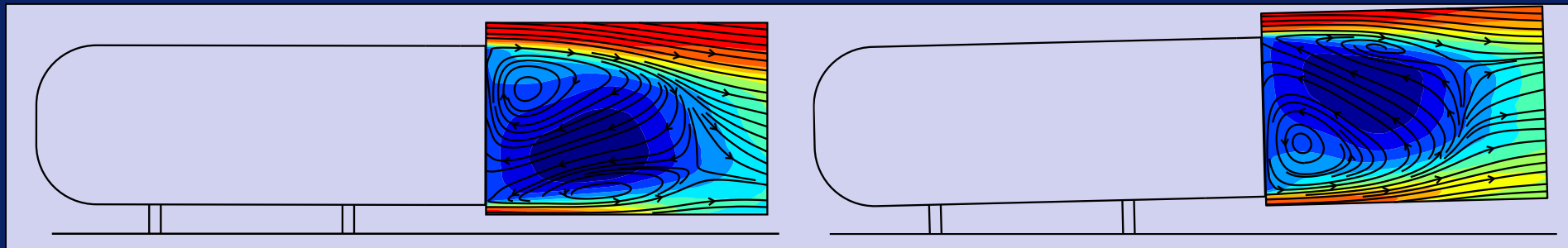


UNIVERSITY OF
LIVERPOOL

Mean structure of the recirculating flow at the rear of a 3D blunt body at different attitudes

Olivier Cadot

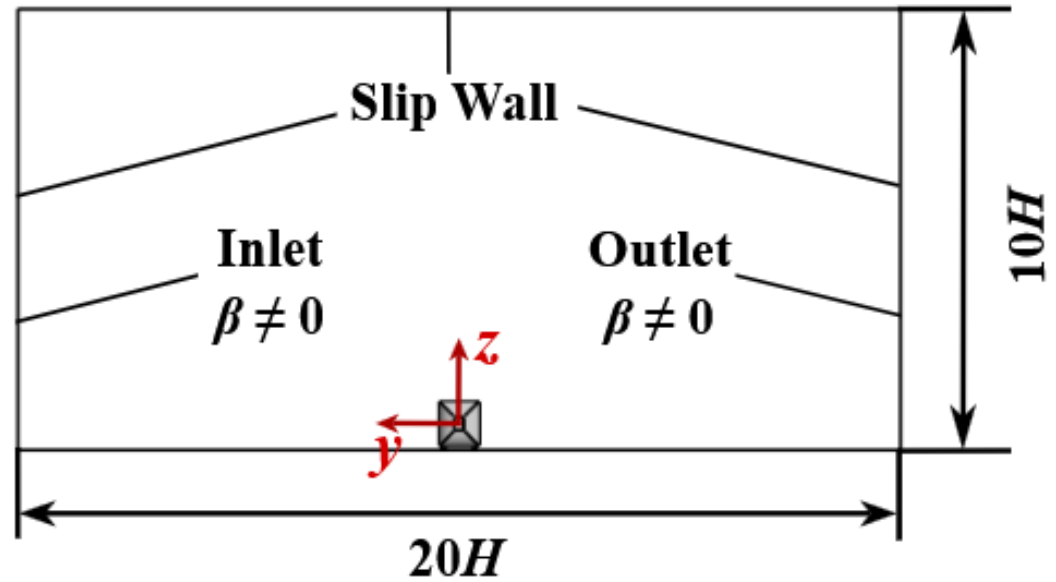
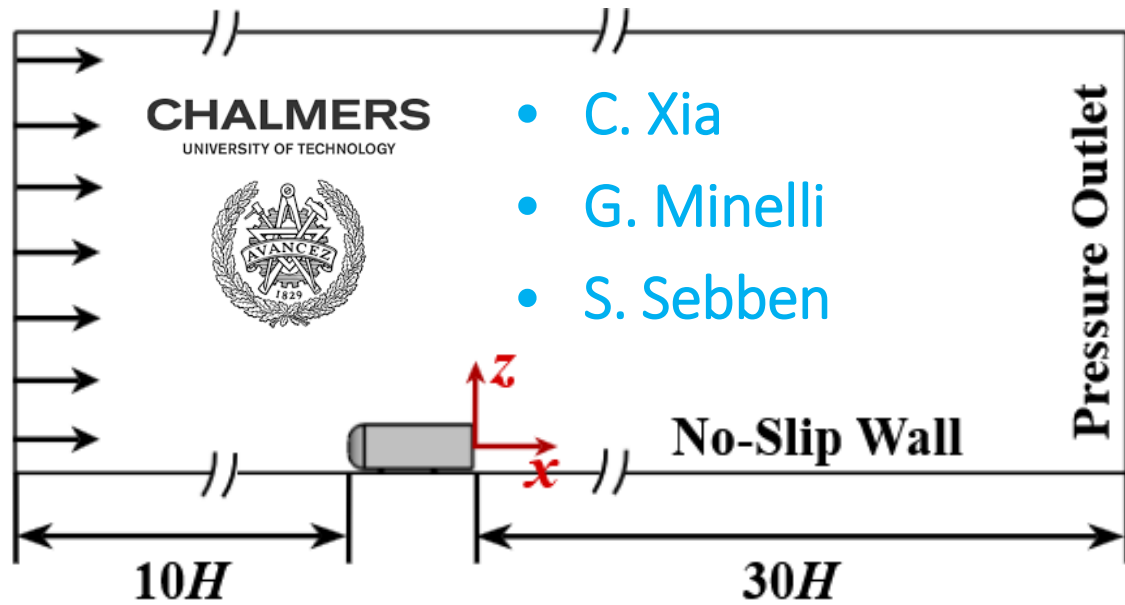
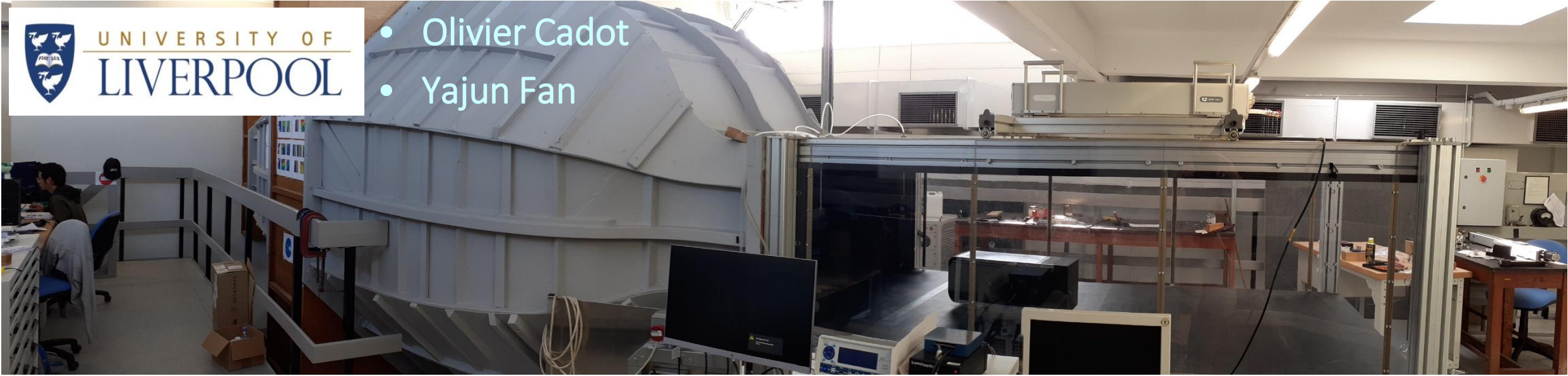
Department of Mechanical and Aerospace Engineering





UNIVERSITY OF
LIVERPOOL

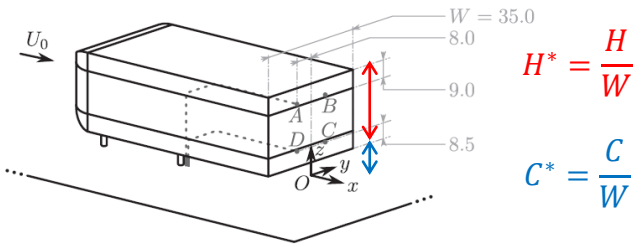
- Olivier Cadot
- Yajun Fan



Summary

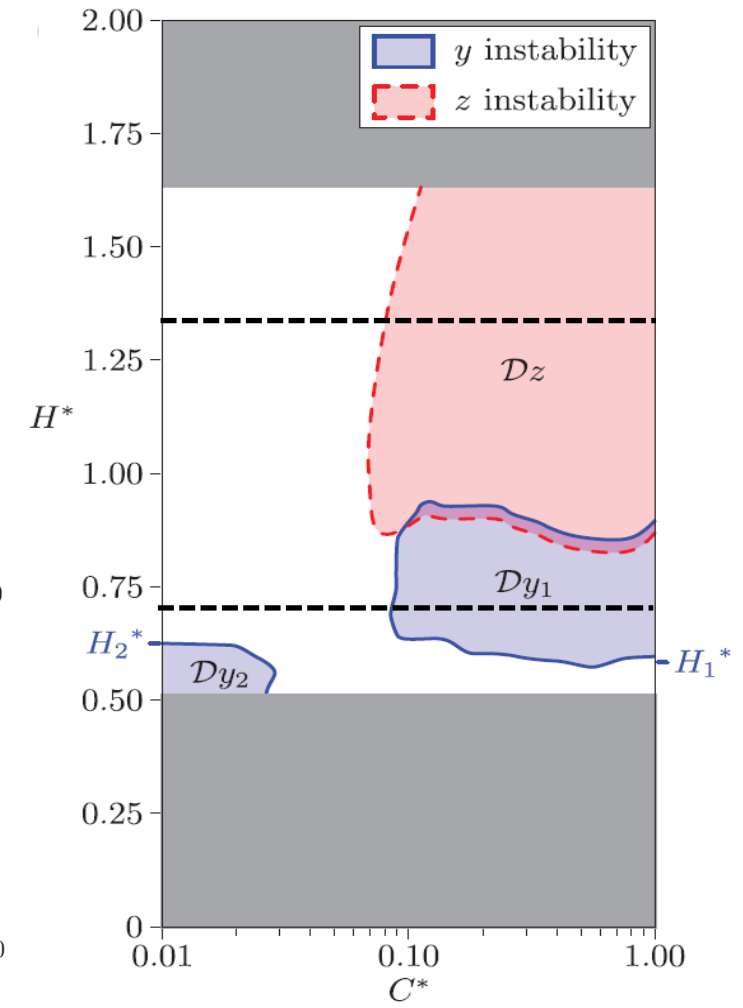
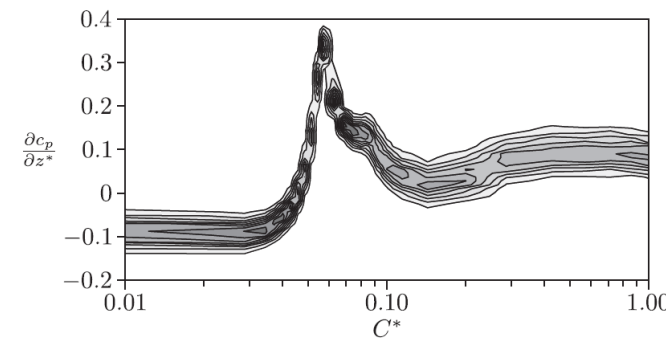
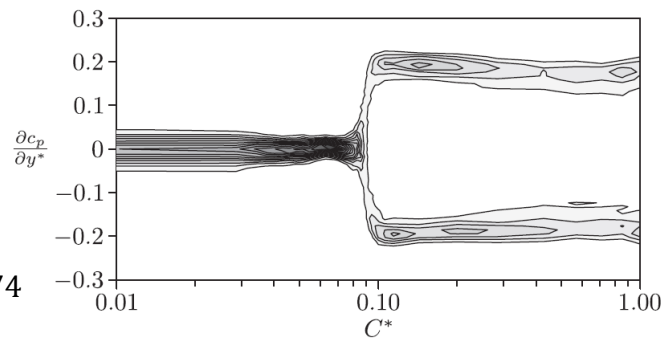
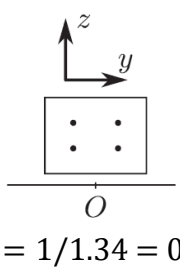
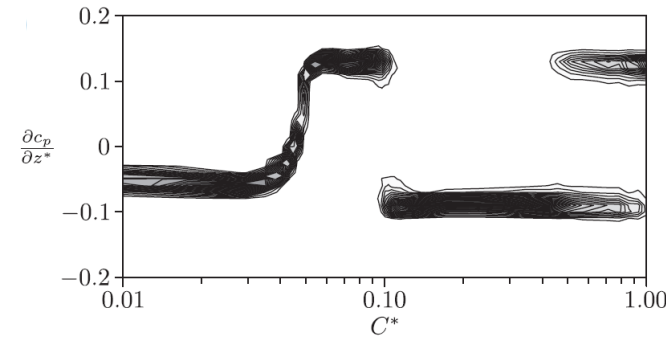
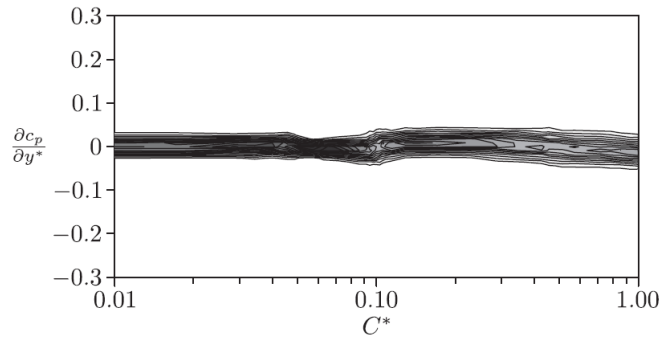
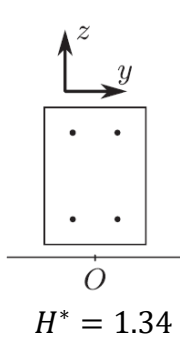
1. Introduction about steady asymmetry and recirculating flow structure of blunt trailing edge bluff-bodies
2. LES and Experiment at different body attitudes
3. Conclusion and perspectives

1. Introduction

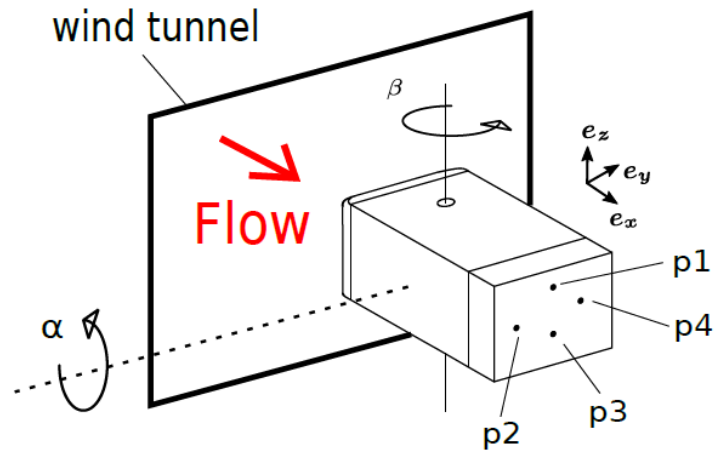


Grandemange, Gohlke & Cadot (PoF 2013)

$$Re = 4.5 \times 10^4$$



Permanent asymmetry when $\frac{2}{3} \leq \frac{H}{W} \leq \frac{3}{2}$

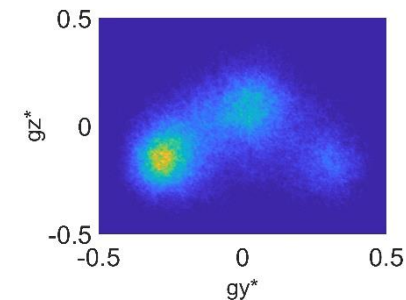
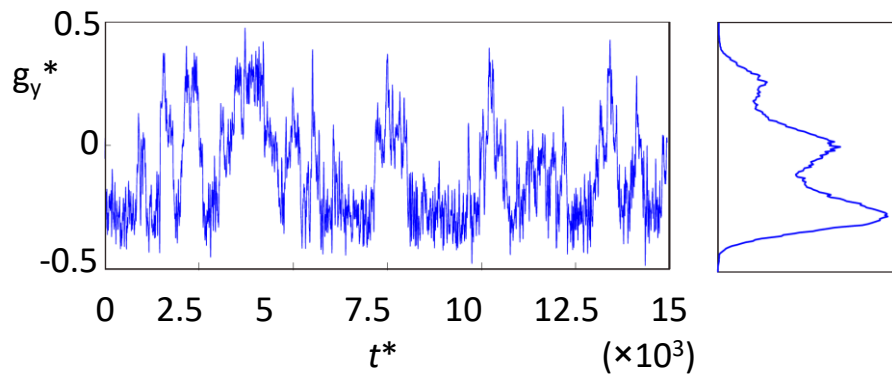
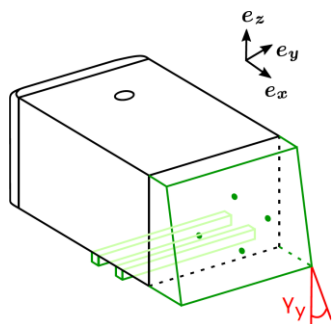
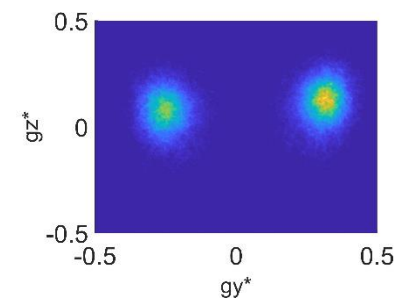
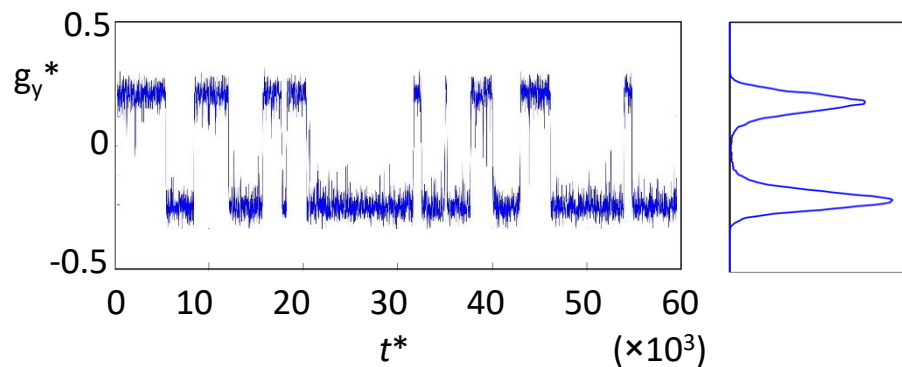
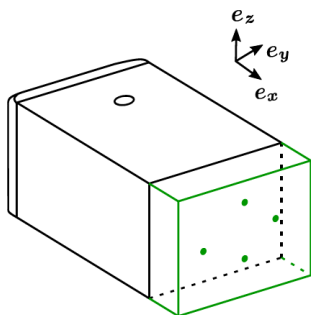


$$g_y^* = \frac{C_{p4} - C_{p2}}{\Delta_y^*}$$

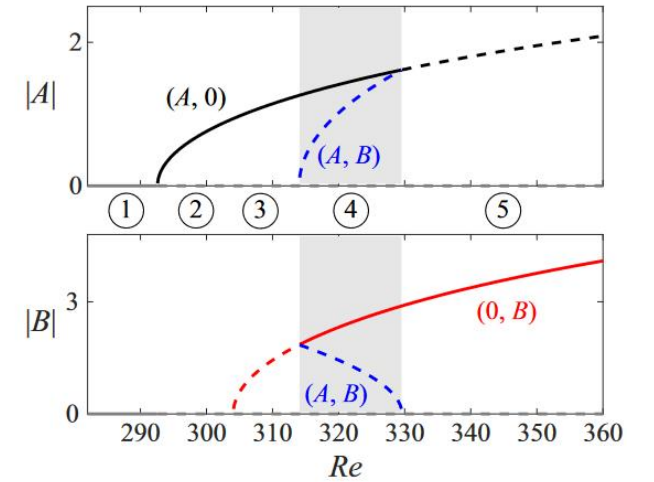
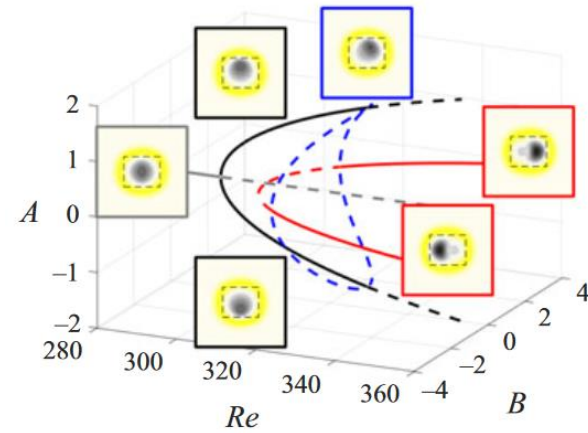
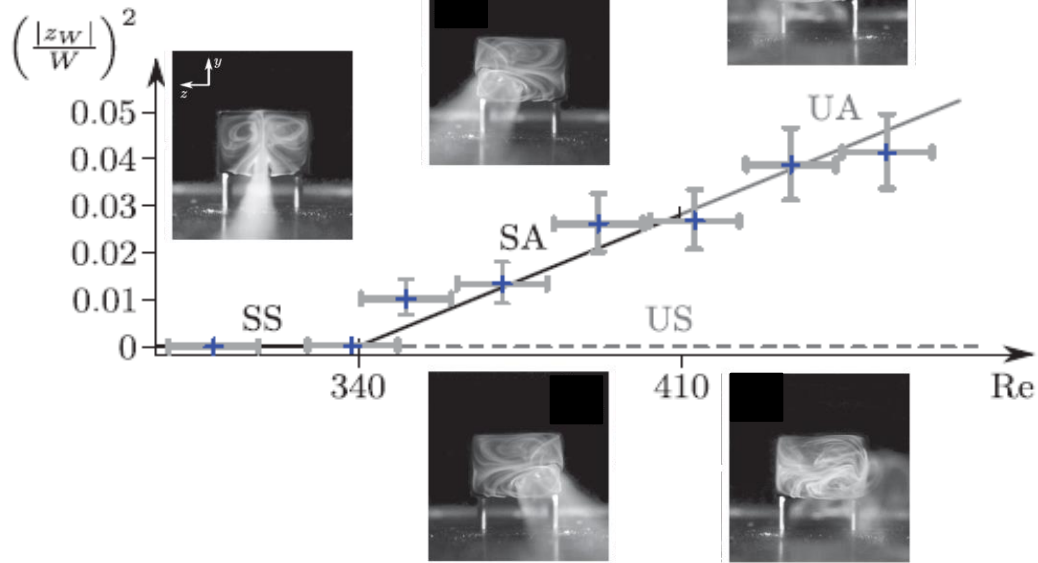
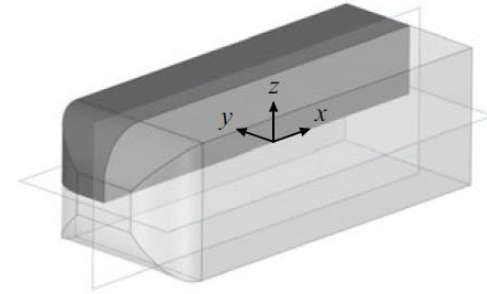
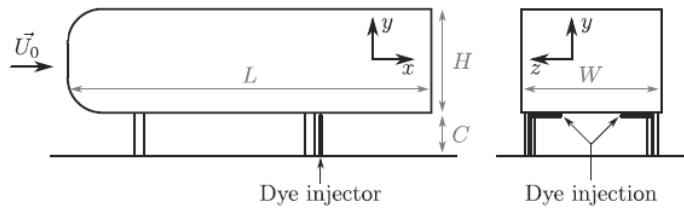
$$g_z^* = \frac{C_{p1} - C_{p3}}{\Delta_z^*}$$

$$Re = 2 \times 10^5$$

Legai & Cadot (ExiF 2020)

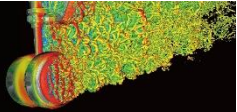


UNIVERSITY OF
LIVERPOOL



Grandemange, Gohlke & Cadot
(Phys. Rev. E 2012)

Zampogna & Boujo (J. Fluid Mech 2023)



Krajnovic & Davidson (JFE 2003)

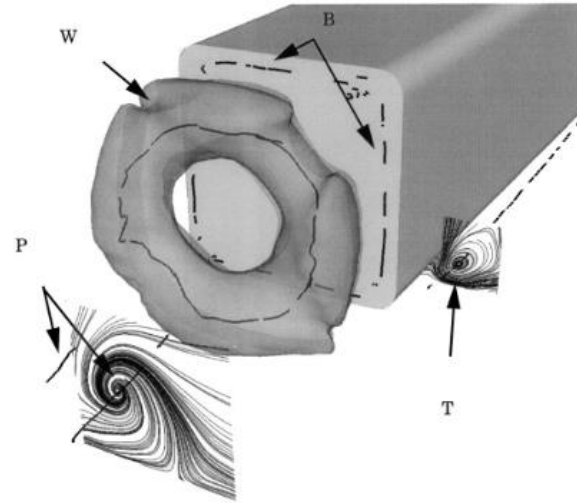
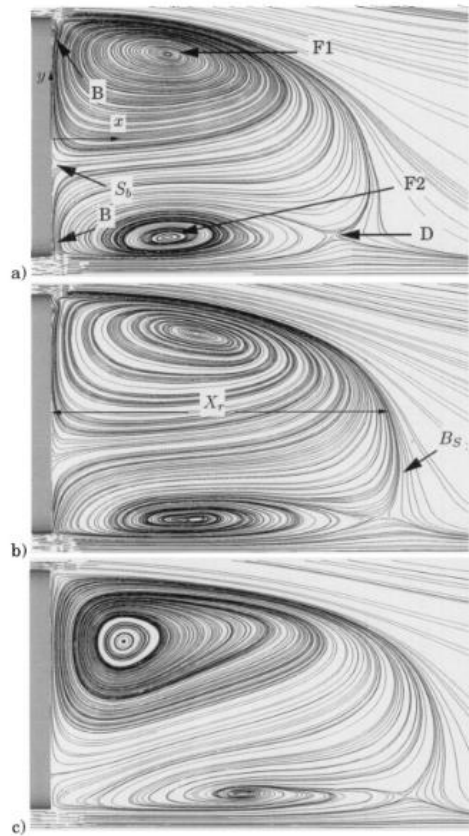
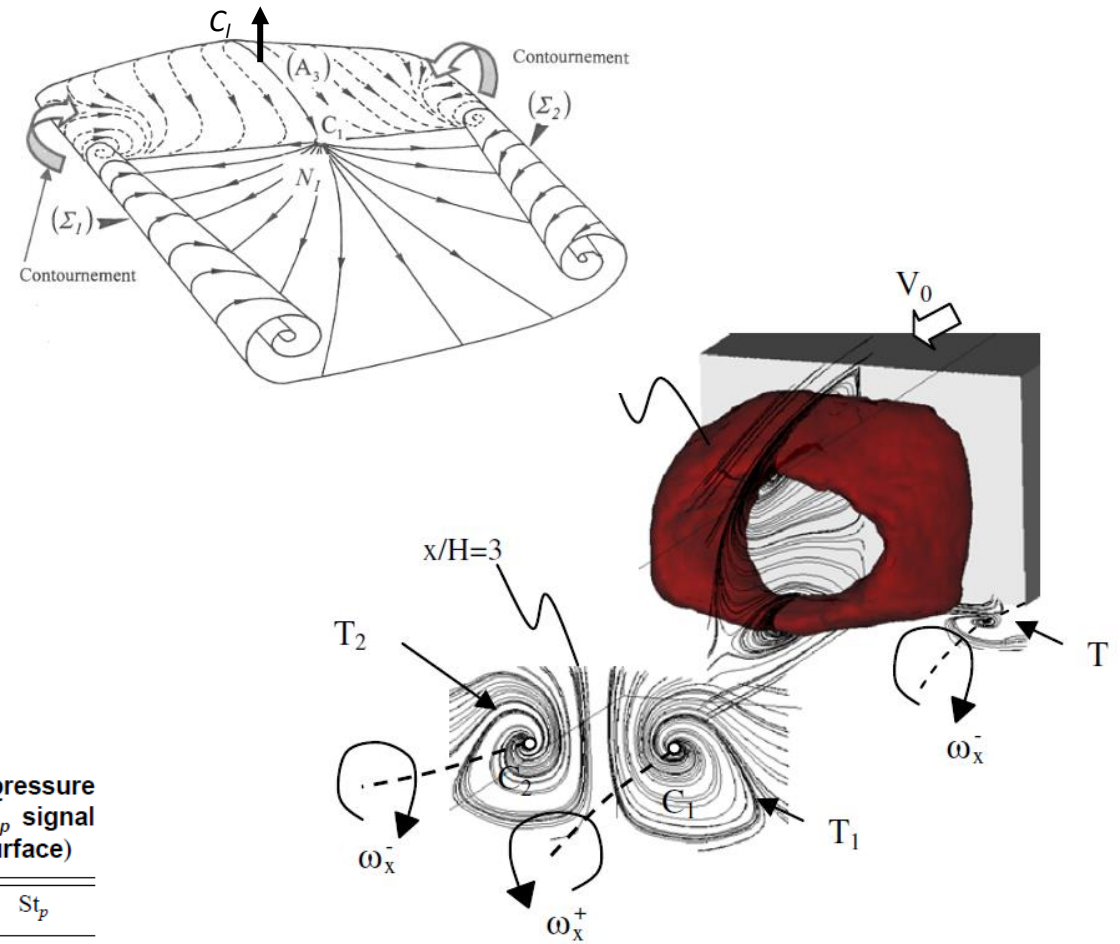


Fig. 10 The isosurface of time-averaged pressure $p=-0.20$. The black curves represent the vortex cores of the thin edge vortices B , the ring vortex W , and the longitudinal vortices behind the separation bubble P . Vortices on the right side ($z < 0$), P and T , are visualized using streamlines in planes $x = 1.4H$ and $x = -0.48H$, respectively (note that the mirror image vortices on the left side, i.e., $z > 0$, are not shown in this figure). View of the rear face of the body.

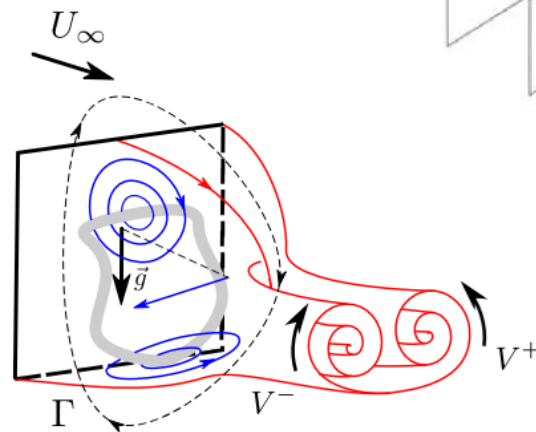
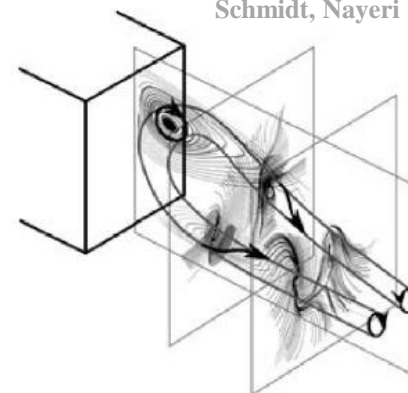
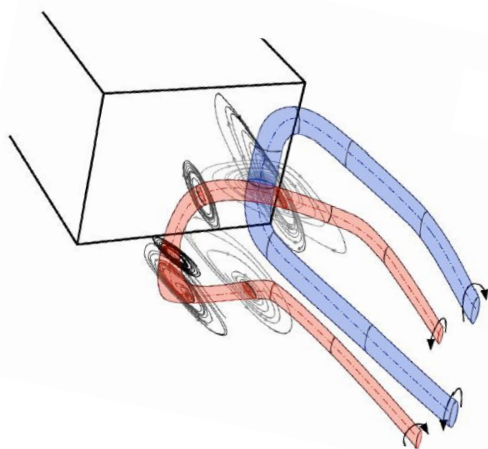
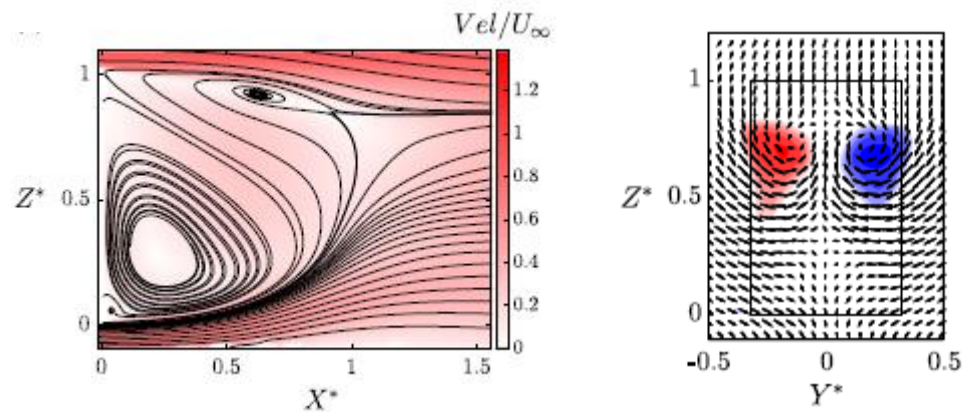
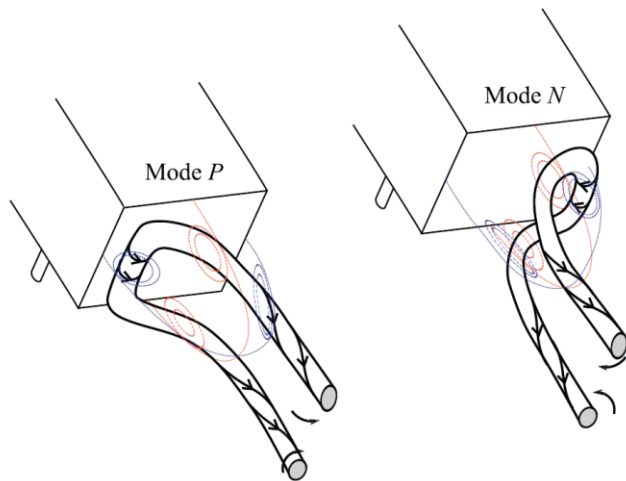
Table 3 Time-averaged pressure drag, lift, and rear pressure coefficients and dominating frequency (St_p) of the C_p signal (note that \bar{C}_p means the integrated C_p over the rear surface)

Case	$\langle C_D \rangle_t$	$\langle C_L \rangle_t$	$\langle \bar{C}_p \rangle_t$	St_p
Coarse	0.206	-0.066	-0.216	0.073
Medium	0.318	-0.066	-0.224	0.055
Fine	0.33	-0.071	-0.229	0.059

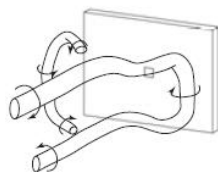
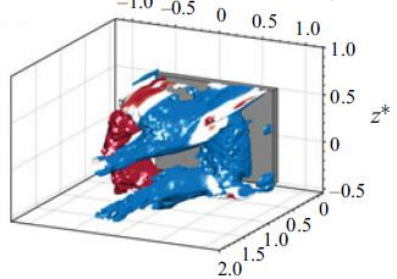
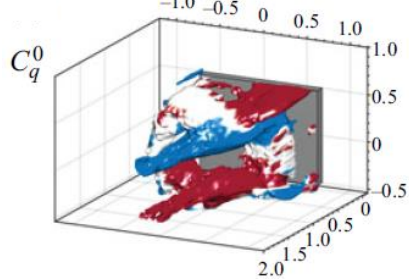
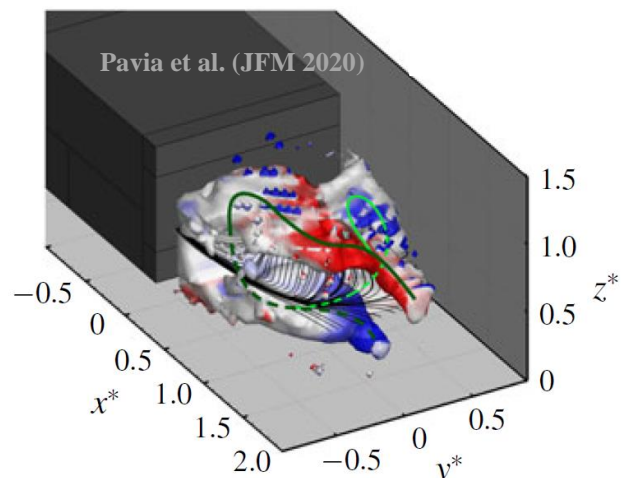


Rouméas, Gilliéron & Kourta (C&F 2008)





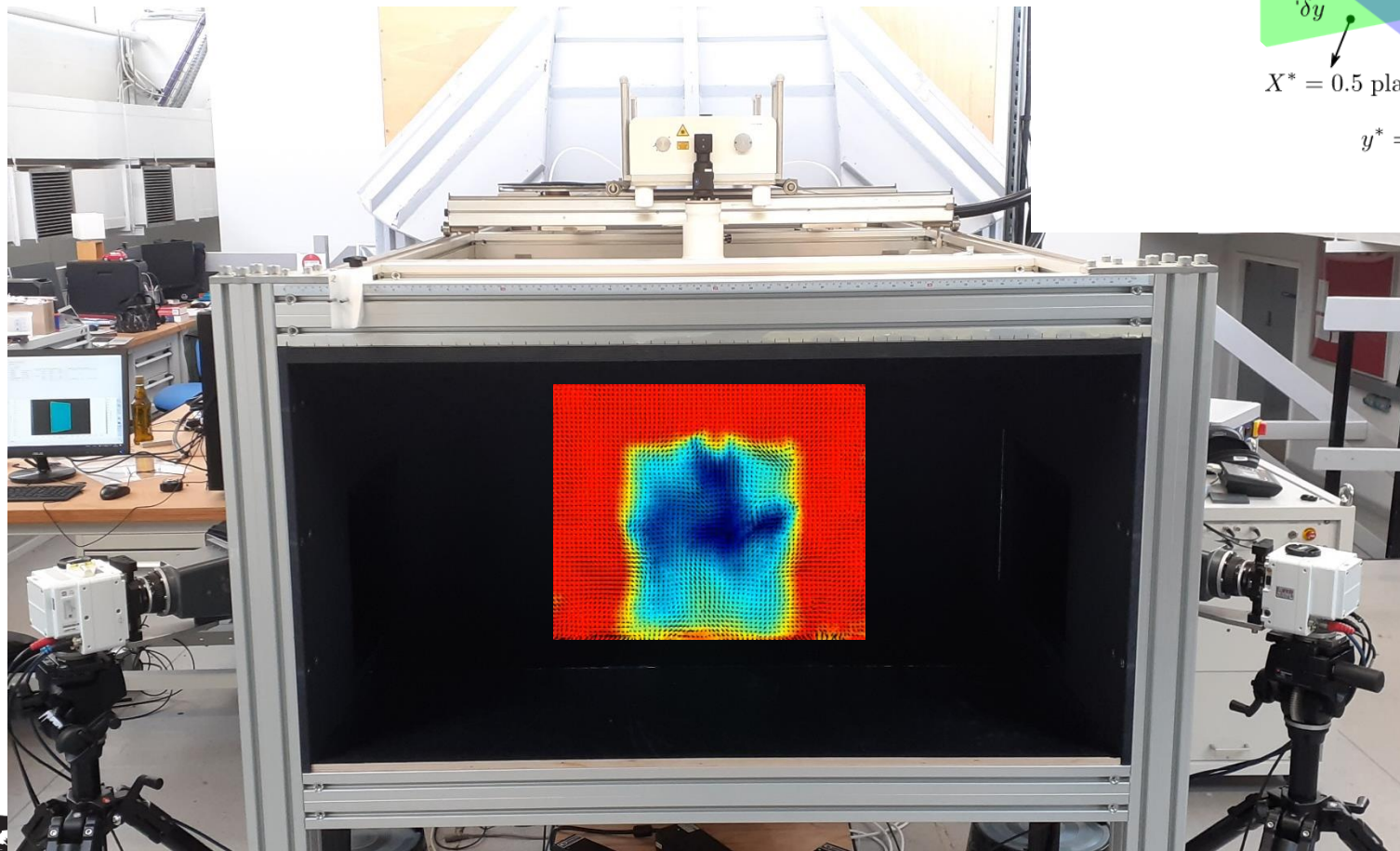
Our proposition ...



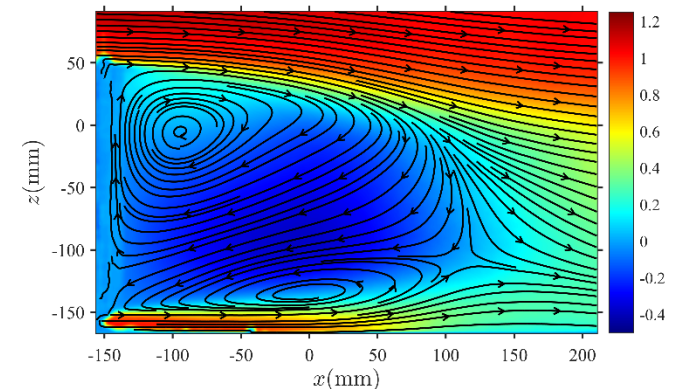
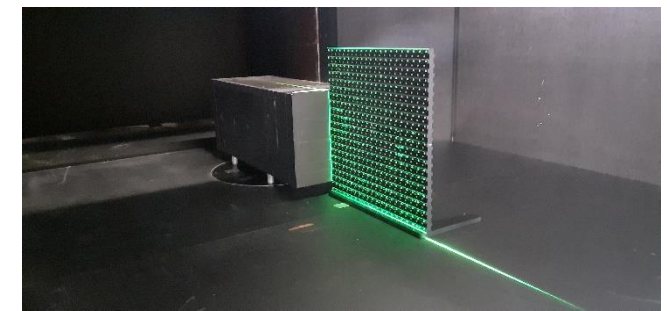
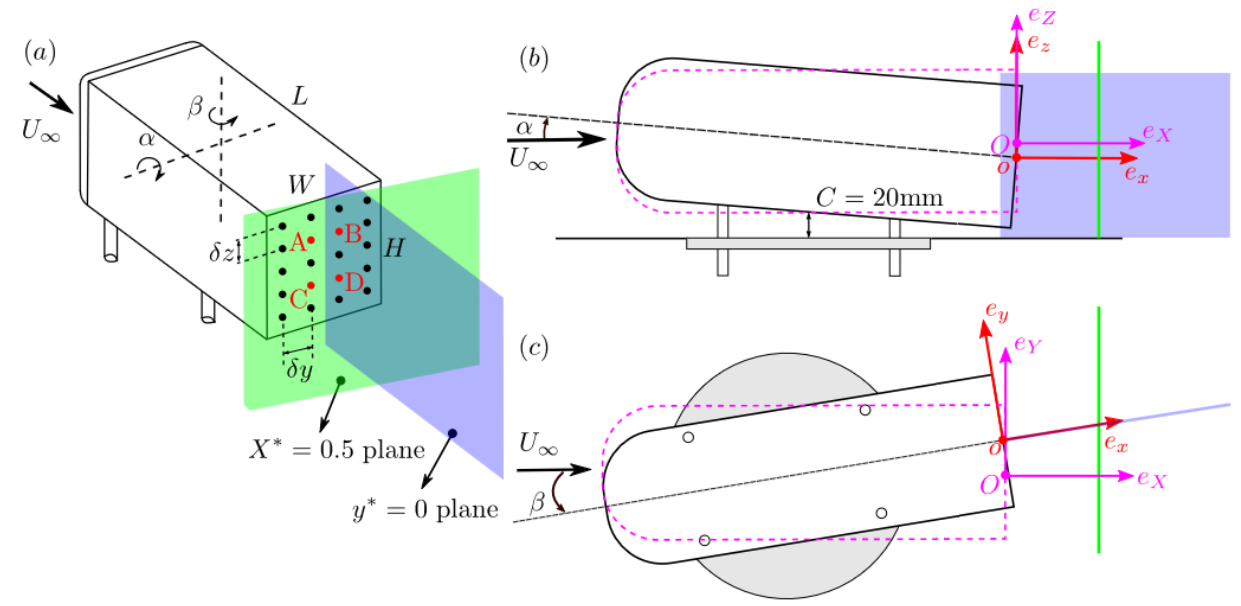
2. A complementary study of experiment and LES

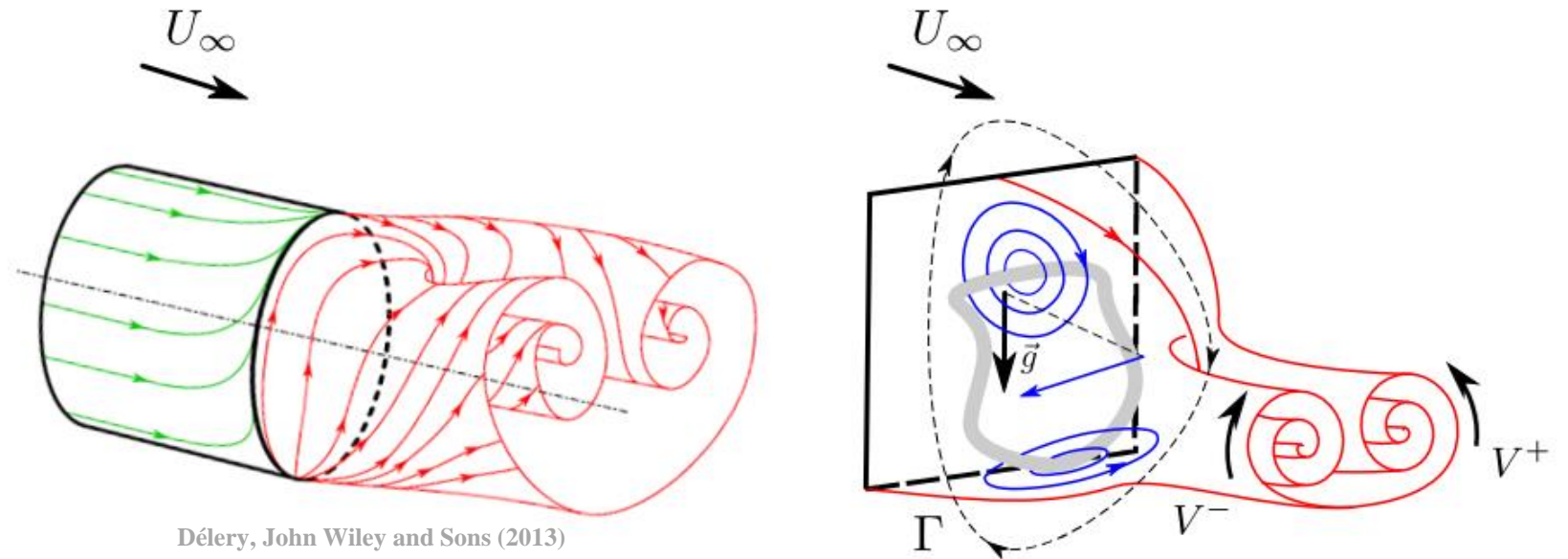
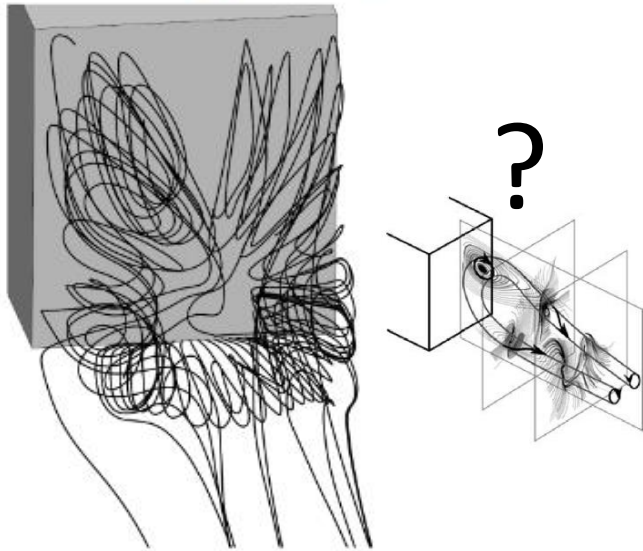
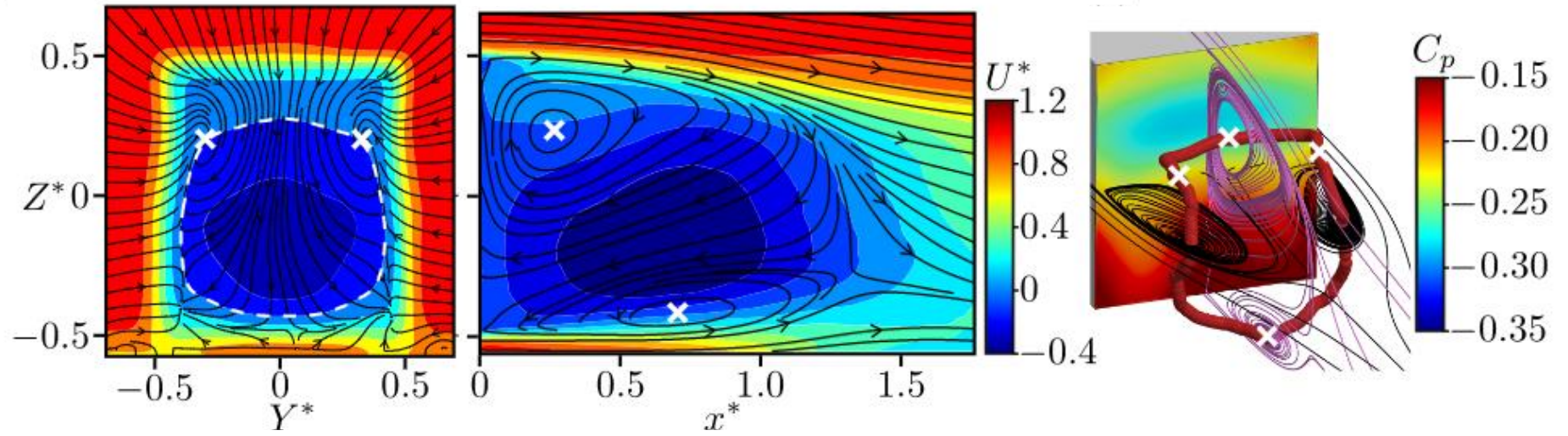
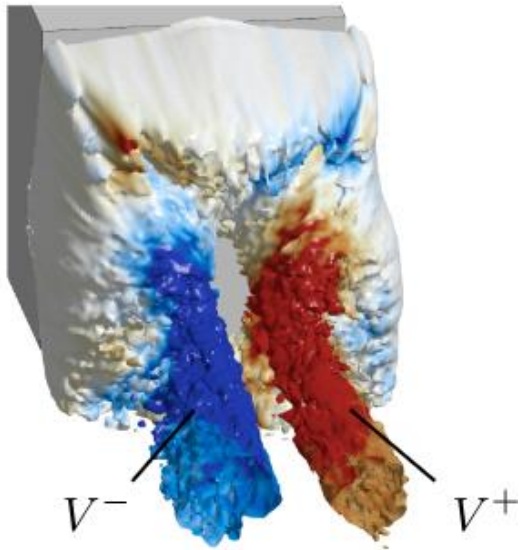
Fan, Parezanovic & Cadot (JFM 2022)

Fan, Xia, Minelli, Sebben & Cadot (Submitted to JFM 2025)



LIVERPOOL



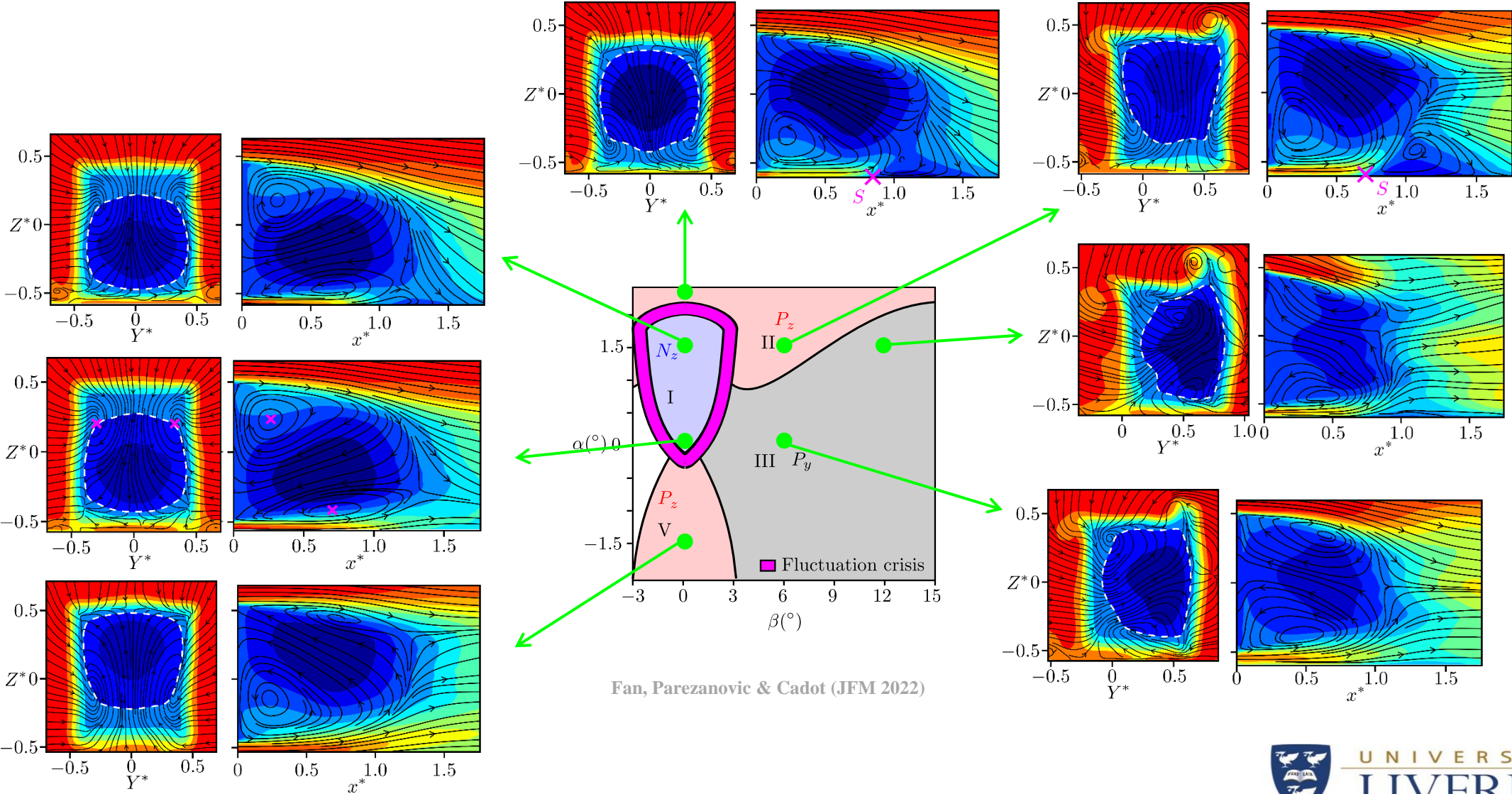


Déleury, John Wiley and Sons (2013)

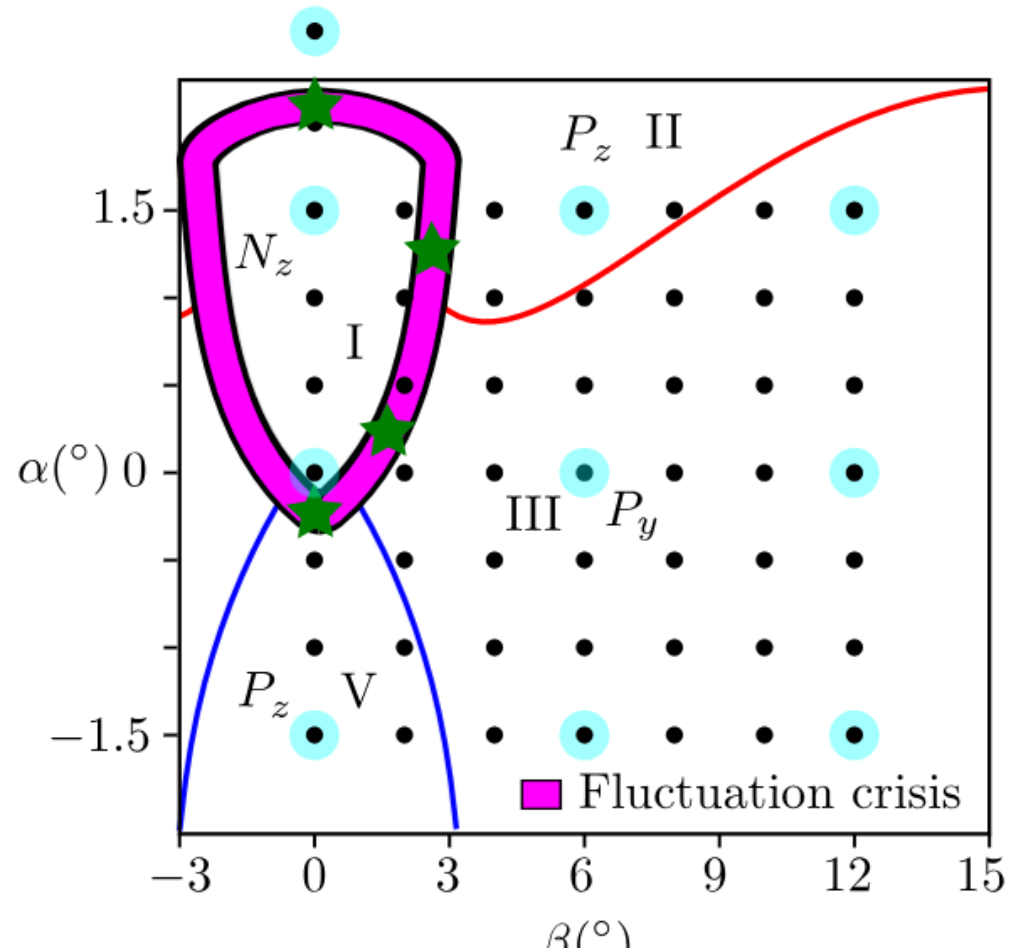
The asymmetric structure can increase or reduce the lift on the body through the vertical pressure gradient \vec{g} .



Change of body attitude



Fan, Parezanovic & Cadot (JFM 2022)



- mean flow investigation
- ★ wake transition investigation
- LES investigation



UNIVERSITY OF
LIVERPOOL

Attitude (β, α)	C_i/C_i^{WT}	C_x	C_x^{LES}	C_b	C_b^{LES}	C_y	C_y^{LES}	C_z	C_z^{LES}
$(0^\circ, -1.5^\circ)$	0.895	0.321	0.318	0.222	0.225	0.005	0.000	-0.287	-0.420
$(0^\circ, 0^\circ)$	0.901	0.301	0.306	0.206	0.217	0.002	0.001	-0.095	-0.176
$(0^\circ, 1.5^\circ)$	0.896	0.320	0.322	0.218	0.229	0.001	0.000	0.052	0.019
$(0^\circ, 2.6^\circ)$	0.891	0.340	0.330	0.226	0.228	-0.015	-0.002	0.185	0.244
$(6^\circ, -1.5^\circ)$	0.868	0.348	0.341	0.257	0.262	-0.461	-0.507	-0.274	-0.389
$(6^\circ, 0^\circ)$	0.872	0.348	0.341	0.257	0.272	-0.475	-0.508	-0.088	-0.179
$(6^\circ, 1.5^\circ)$	0.868	0.341	0.325	0.248	0.252	-0.459	-0.495	0.078	0.034
$(12^\circ, -1.5^\circ)$	0.843	0.372	0.363	0.323	0.343	-0.962	-1.059	-0.216	-0.380
$(12^\circ, 0^\circ)$	0.848	0.373	0.350	0.321	0.335	-0.973	-1.066	0.014	-0.088
$(12^\circ, 1.5^\circ)$	0.843	0.381	0.350	0.318	0.328	-0.982	-1.083	0.249	0.221

TABLE 2. Force component and base suction coefficients obtained for the experiment with the correction factor C_i/C_i^{WT} (see Eq.2.6) and the LES at different body attitudes.

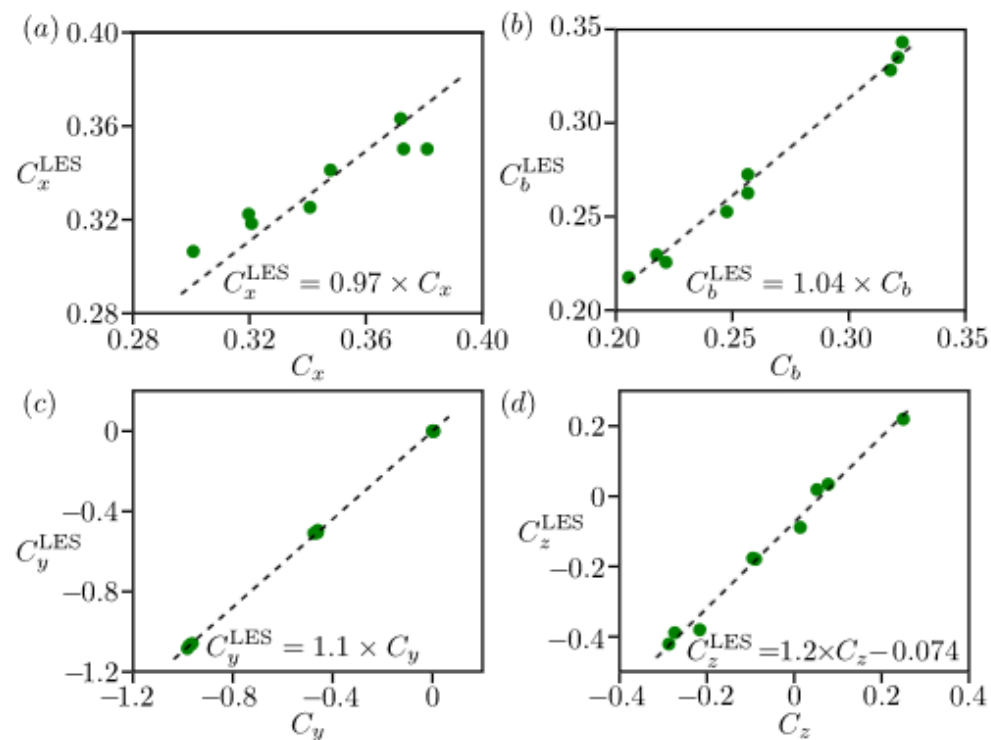
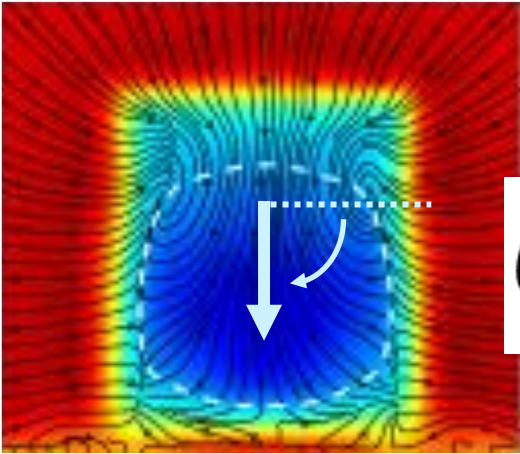


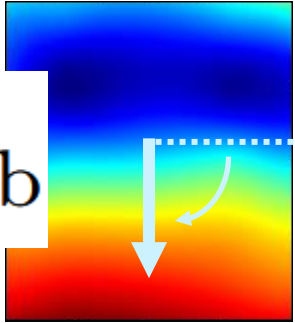
FIGURE 5. Comparison of the aerodynamic coefficients obtained from the experiment and the LES for: (a) drag; (b) base suction; (c) side force and (d) lift.

Wake orientation in attitude space

Reverse cross-flow angle



Base pressure gradient angle

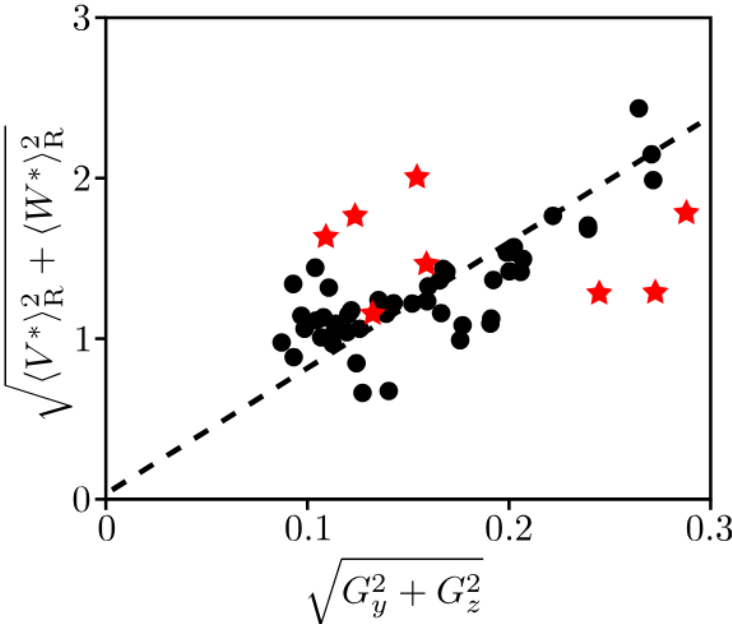
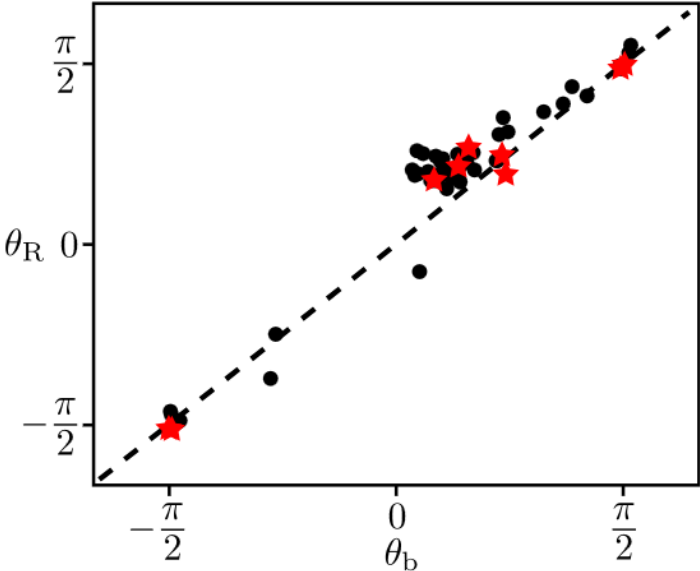
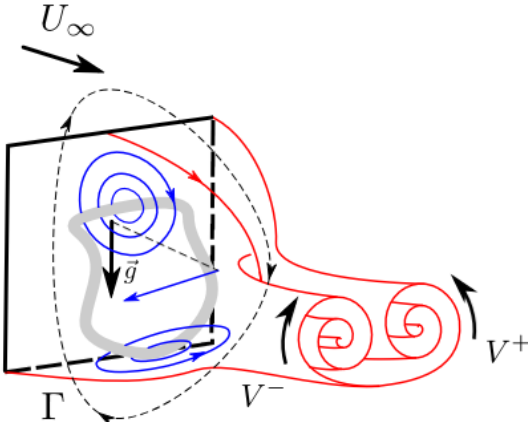


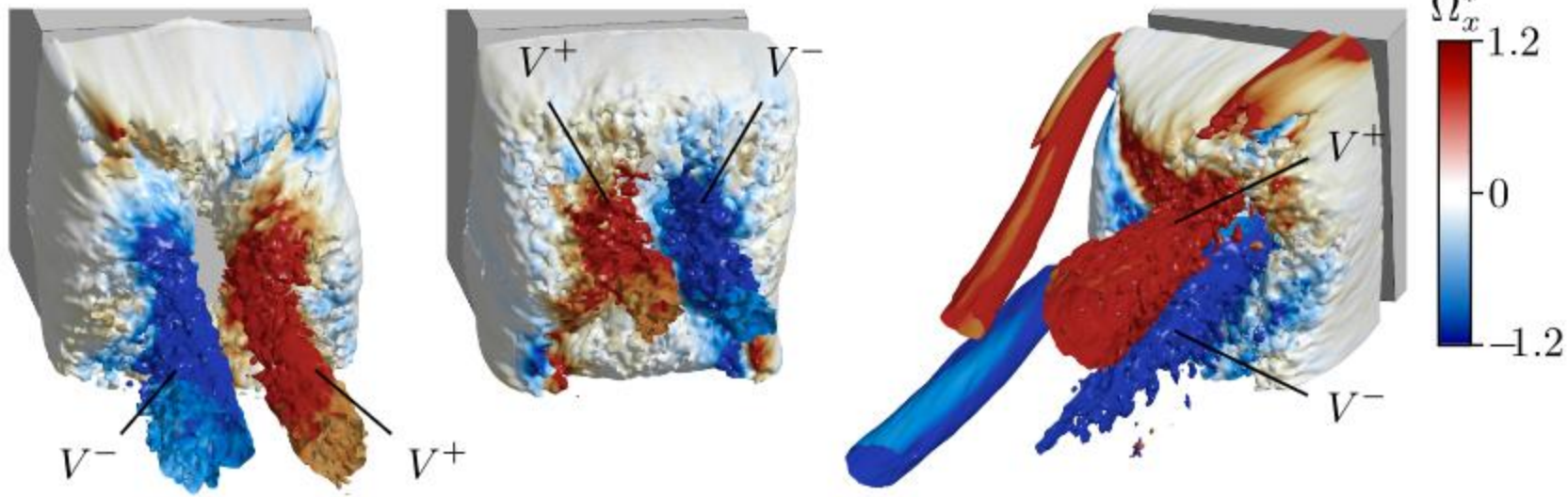
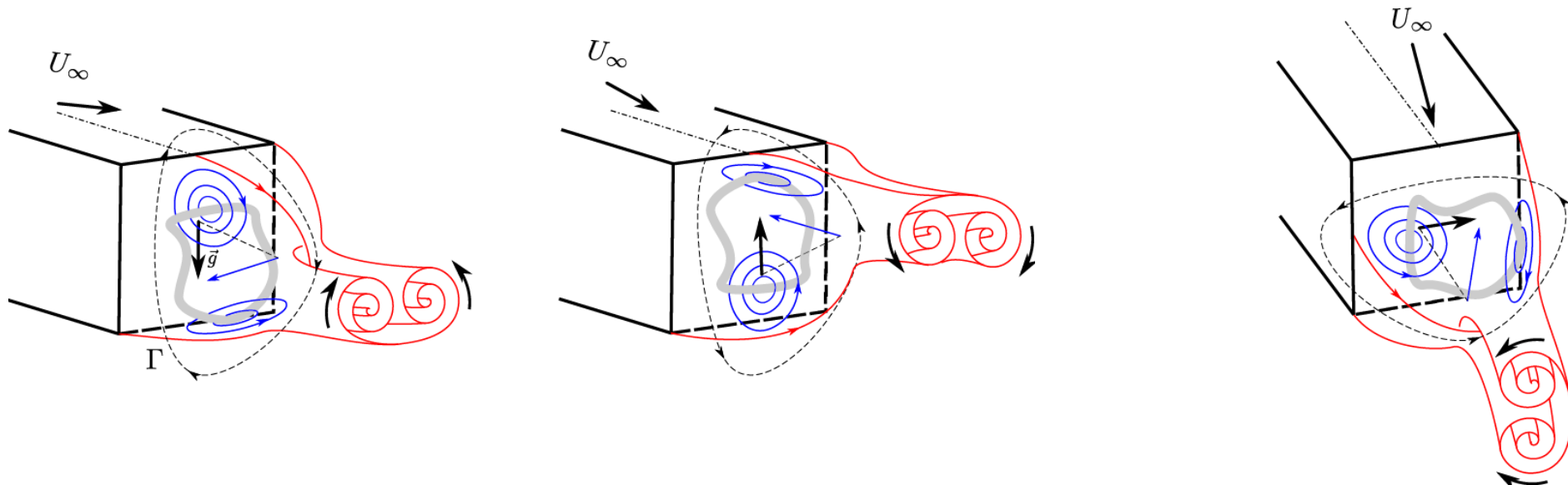
$$\theta_R \approx \theta_b$$

$$\theta_b = \arctan \frac{G_z}{G_y}$$

$$\langle W \rangle_{U < 0} \quad \langle V \rangle_{U < 0}$$

$$\theta_R = \arctan \frac{\langle W^* \rangle_R}{\langle V^* \rangle_R}$$



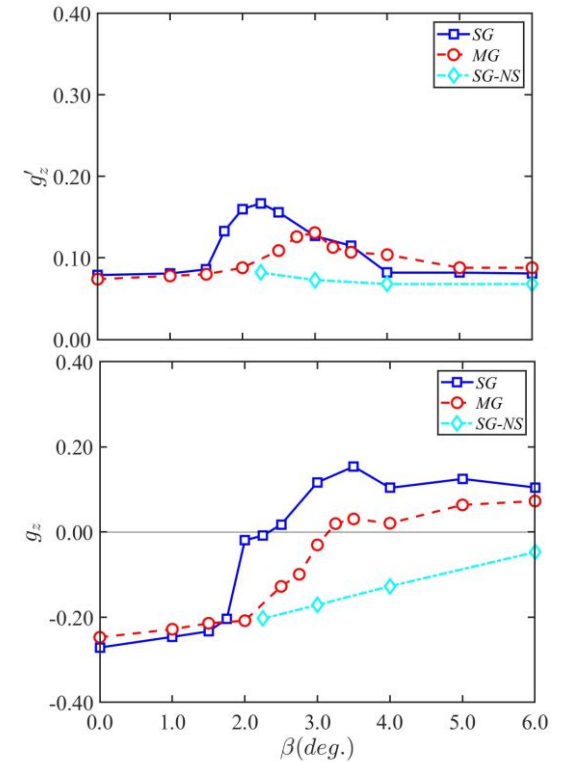
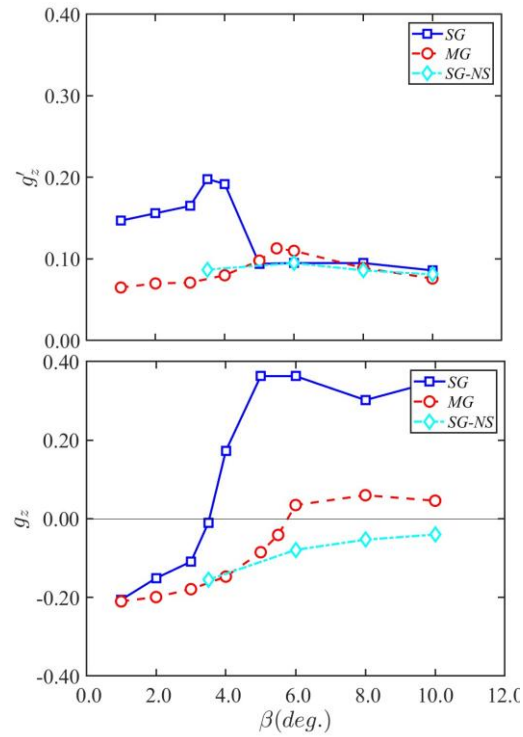
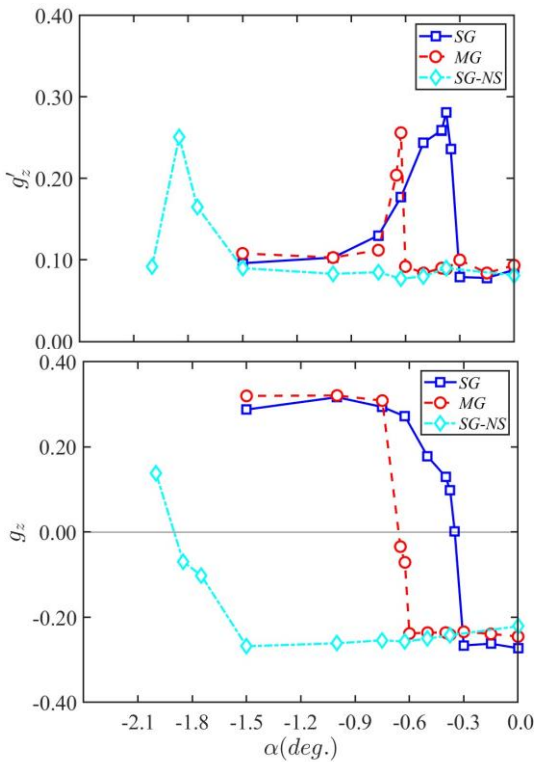
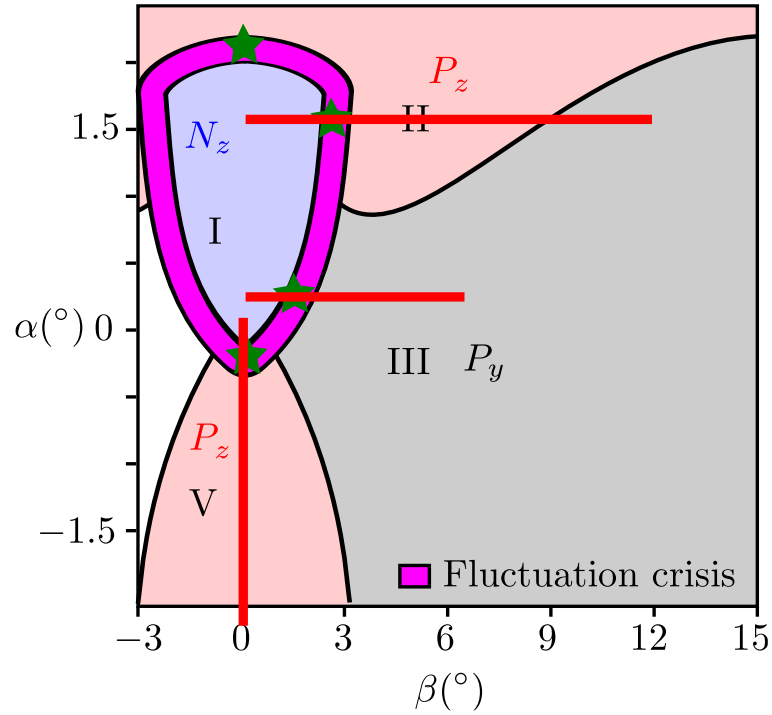


6. Conclusion and perspectives

- A 3D structure of the recirculating flow is proposed :
 - The recirculating flow is subjected to a steady instability leading to an asymmetry towards the major axis of the base
 - This asymmetry is associated with a circulation provoking the closure of the separated surface into two longitudinal vortices
- The LES will be applied to a moving ground (real boundary condition for ground vehicles)

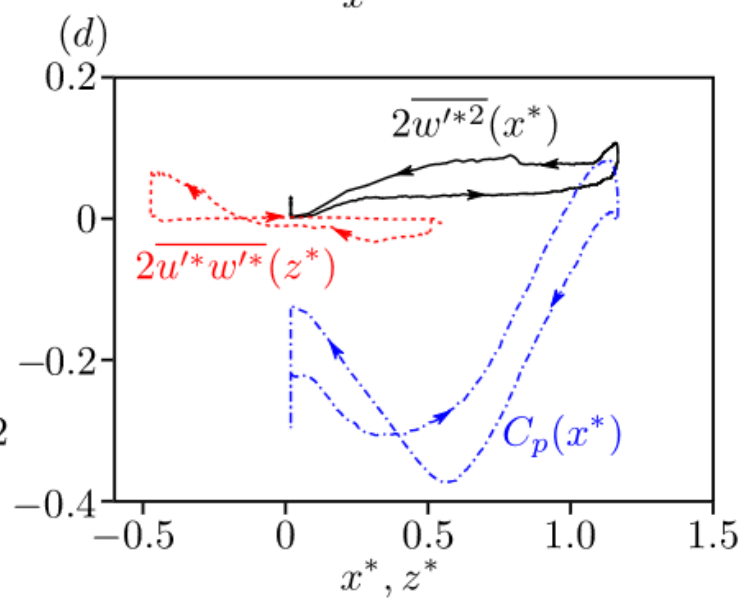
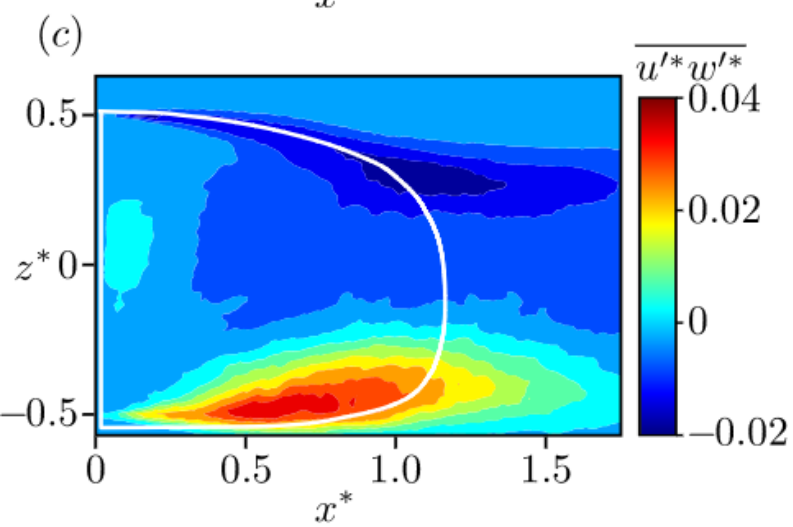
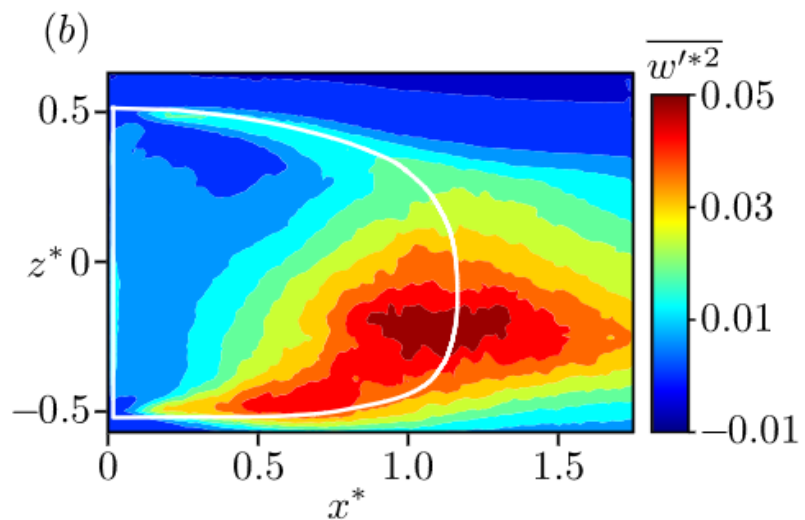
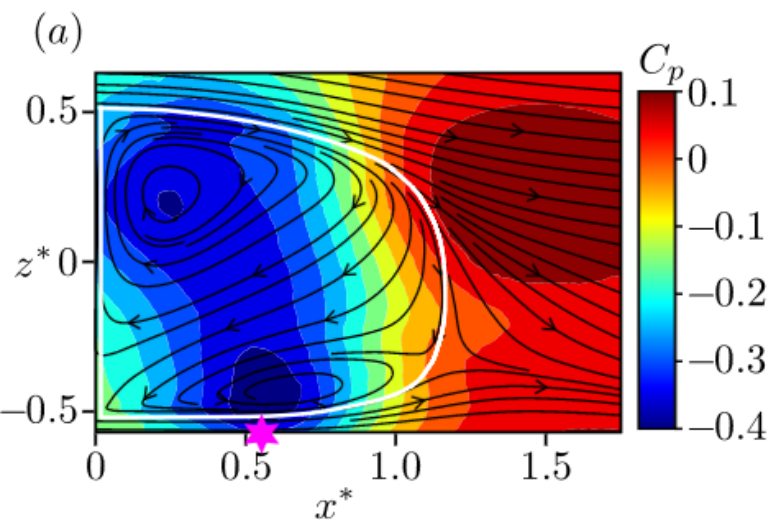
Role of static ground and supports

- Static Ground (SG)
- Moving Ground (MG)
- ◇ Static Ground No supports (SG-NS)



Separatrix equilibrium

$$-\oint_{\mathcal{C}} C_p dx^* - \oint_{\mathcal{C}} 2\overline{w'^*{}^2} dx^* - \oint_{\mathcal{C}} 2\overline{u'^*w'^*} dz^* = 0,$$



Ground separation

- Boundary layer (static floor)
- Adverse pressure gradient

